SANDIA REPORT

SAND2008-7895
Unlimited Release
Printed December 2008

Use of Ceragenins To Create Novel Biofouling Resistant Water-Treatment Membranes

Susan J. Altman, Michael Hibbs, Howland D. T. Jones, Paul B. Savage, Lucas K. McGrath, Andres L. Sanchez, Benjamin D. Fellows, Jacob Pollard and Yanshu Feng

Prepared by
Sandia National Laboratories
Albuquerque, New Mexico 87185 and Livermore, California 94550

Sandia is a multiprogram laboratory operated by Sandia Corporation, a Lockheed Martin Company, for the United States Department of Energy's National Nuclear Security Administration under Contract DE–AC04–94AL85000.

Issued by Sandia National Laboratories, operated for the United States Department of Energy by Sandia Corporation.

Available to DOE and DOE contractors from
U.S. Department of Energy
Office of Scientific and Technical Information
P.O. Box 62
Oak Ridge, TN 37831

Telephone: (865)576–8401
Facsimile: (865)576–5728
E–Mail: reports@adonis.osti.gov
Online ordering: http://www.doe.gov/bridge

Available to the public from
U.S. Department of Commerce
National Technical Information Service
5285 Port Royal Rd
Springfield, VA 22161

Telephone: (800)553–6847
Facsimile: (703)605–6900
E–Mail: orders@ntis.fedworld.gov
Online order: http://www.ntis.gov/ordering.htm

SAND2008–7895
Unlimited Release
Printed December 2008

Use of Ceragenins To Create Novel Biofouling Resistant Water-Treatment Membranes

Susan J. Altman[1], Michael Hibbs[2], Howland D. T. Jones[3], Paul B. Savage[4], Lucas K. McGrath[5], Andres L. Sanchez[5], Benjamin D. Fellows[1], Jacob Pollard[4], and Yanshu Feng[4]

[1]Geochemistry Department

[2]Fuels and Energy Transitions Department

[3]Biomolecular Analysis and Imaging Department

Sandia National Laboratories
P.O. Box 5800
Albuquerque, NM 87185

[4]Department of Chemistry and Biochemistry
Brigham Young University
C-100 BNSN
Provo, Utah 84602-5700

[5]LMATA
P.O. Box 5800, MS0754
Albuquerque, NM 87185

Abstract

Scoping studies have demonstrated that ceragenins, when linked to water-treatment membranes have the potential to create biofouling resistant water-treatment membranes. Ceragenins are synthetically produced molecules that mimic antimicrobial peptides. Evidence includes measurements of CSA-13 prohibiting the growth of and killing planktonic *Pseudomonas fluorescens*. In addition, imaging of biofilms that were in contact of a ceragenin showed more dead cells relative to live cells than in a biofilm that had not been treated with a ceragenin. This work has demonstrated that ceragenins can be attached to polyamide reverse osmosis (RO) membranes, though work needs to improve the uniformity of the attachment. Finally, methods have been developed to use hyperspectral imaging with multivariate curve resolution to view ceragenins attached to the RO membrane. Future work will be conducted to better attach the ceragenin to the RO membranes and more completely test the biocidal effectiveness of the ceragenins on the membranes.

This page is intentionally left blank

ACKNOWLEDGMENTS

This research was funded by the Sandia National Laboratories Laboratory Directed Research and Development (LDRD) program, Senior Council Tier 1 Investment Area.

This page is intentionally left blank

CONTENTS

LIST OF TABLES

LIST OF FIGURES

1 INTRODUCTION

Biofouling impacts membrane separation processes for many industrial applications such as desalination[*Watson et al.*, 2003], waste-water treatment [*Ridgway et al.*, 1983], oil and gas extraction, and power generation. For example, in one desalination pilot plant using nanofilturation membranes, the normalized pressure drop (actual pressure drop normalized for flow and temperature) increased from about 200 to 400 kPa within a two-week period [*Vrouwenvelder et al.*, 1998]. Biological analysis of the membranes show high biofilm densities on the feed side of the spiral wound membrane elements. *Ridgway et al.* [1983] give evidence of microbial fouling in Water Factory 21, a waste-water treatment facility in Southern California. Biofouling results in a loss of permeate flux and increase in energy use. Biofouling becomes an issue in the energy sector as water recycling becomes more and more prevalent. Examples include re-use of cooling water and water used for steam injection for heavy oil extraction. Other sectors that need ultrapure water, such as pharmaceuticals and the microchips and electronics industries, can also benefit from biofouling resistant membranes.

We present preliminary investigations on the ability of ceragenins to create biofouling resistant water-treatment membranes. Ceragenins are synthetically produced molecules that mimic antimicrobial peptides [*Savage*, 2002]. Humans have an innate immune system comprised of, in part, antimicrobial peptides capable of the detection, prevention and fighting of bacterial infections. The characteristics of these peptides is that there is little likelihood that they will develop resistance, they are capable of rapidly killing target organisms, they have a broad spectrum of activity and they are selectively toxic to prokaryotic cells over eukaryotic cells (e.g., bacteria over human cells). However, despite these promising attributes, there are considerable challenges in the clinical application of candidate peptide therapies [*Jenssen et al.*, 2006].

Paul Savage invented the synthetic molecule that mimics the antimicrobial peptides, ceragenins [*Savage et al.*, 2002]. They also display broad-spectrum bactericidal activity against Gram-positive and -negative organisms, including drug resistant bacteria. They are simple to prepare and purify on a large scale and are amenable to broad usage because it is anticipated that they will not engender resistance. They have been incorporated into catheter segments to prevent adherence of organisms. Polymeric forms of ceragenins have also been incorporated into medical devices for sustained release to prevent infection.

Use of ceragenins on water-treatment membranes has not been investigated. Creation of biofouling resistant membranes will assist in creation of clean water and energy with lower energy usage. Ceragenins are synthetically produced antimicrobial peptide mimics that display broad-spectrum bactericidal activity. Use of ceragenins on water-treatment membranes is novel.

This report is organized into four sections. Section 1, this section, is the introduction. The synthesis of the ceragenins used in this work as well as the methods for attaching the ceragenins to water-treatment membranes are presented in Section 2. Testing of the biocidal activity of the ceragenins are discussed in Section 3. Finally, Section 4, summarizes the work and discusses future work.

2 CERAGENIN SYNTHESIS AND ATTACHMENT

This section discusses the synthesis of the ceragenins created for this study, CSA-105 and CSA-108. In addition the attachment methods for these ceragenins are included. Finally, a presentation of the imaging of the ceragenins, both alone and attached to the membranes is presented.

2.1 Synthesis of Ceragenins

2.1.1 Background

Paul Savage and his research group have prepared over 100 different ceragenin analogs. The structure of a typical ceragenin, CSA-13, and the starting material, cholic acid, are shown in Figure 1. Ceragenins are based on a steroid core (the system of four fused saturated rings) with several substituents arranged in such a way that one face of the molecule is hydrophilic while the other face is hydrophobic. In the case of CSA-13, it is the three primary amines (which become ammonium salts when protonated) that cause the near face of the molecule to be hydrophilic. It is this arrangement of hydrophilic and hydrophobic regions that enables ceragenins to mimic antimicrobial peptides. The substituent on the upper right corner of a ceragenin (when drawn as CSA-13 is arranged in Figure 1) can be varied without having a large impact on the biocidal activity of the ceragenin. So that region of the molecule will be used as a "handle" for attaching the specific functionalities desired for this project.

2.1.2 Synthesis

This project requires the addition of two new features to the ceragenin core. First, a reactive group is needed to serve as the point of attachment to a tether which will covalently connect the ceragenin to the membrane surface. Second, an attached fluorophore is needed in order to "see" the ceragenin in order to verify that it has been attached to the membrane and to quantify the density of ceragenins present. The Savage group prepared two new ceregenins bearing these features for this project. A connector consisting of two amide groups was used to attach both the reactive attachment group (an allyl group) and the fluorophore, this connector will be referred to

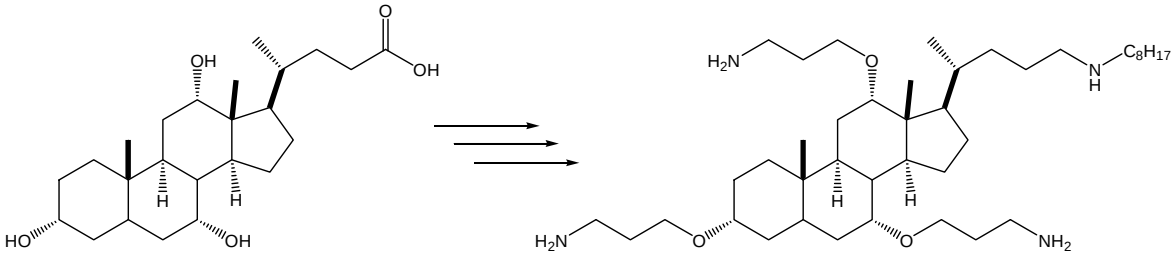

cholic acid CSA-13

Figure 1: A typical ceragenin, CSA-13, and its precursor, cholic acid.

as the "amide connector" for remaining portion of this document. The synthetic schemes are shown in Figures 2 and 3.

In CSA-105, the point of attachment is the terminal alkene and in CSA-108, the point of attachment is the *N*-hydroxysuccinimide ester. After the attachment procedure, the Fmoc groups on the amines on CSA-108 will be removed in a deprotection step with an organic base. In both CSA-105 and CSA-108, the fluorophore is NBD, the heteroatom-containing fused ring system on the right side of both ceregenins as shown in Figures 2 and 3. CSA-109 is the same as CSA-105 without the NBD fluorophore.

2.2 Attachment of Ceragenins

2.2.1 Attachment Procedure

Two different attachment methods were planned for the newly-prepared ceragenins. Method 1 is based on the report of Belfer et al. [1998] in which acrylate-type oligomers were attached to the

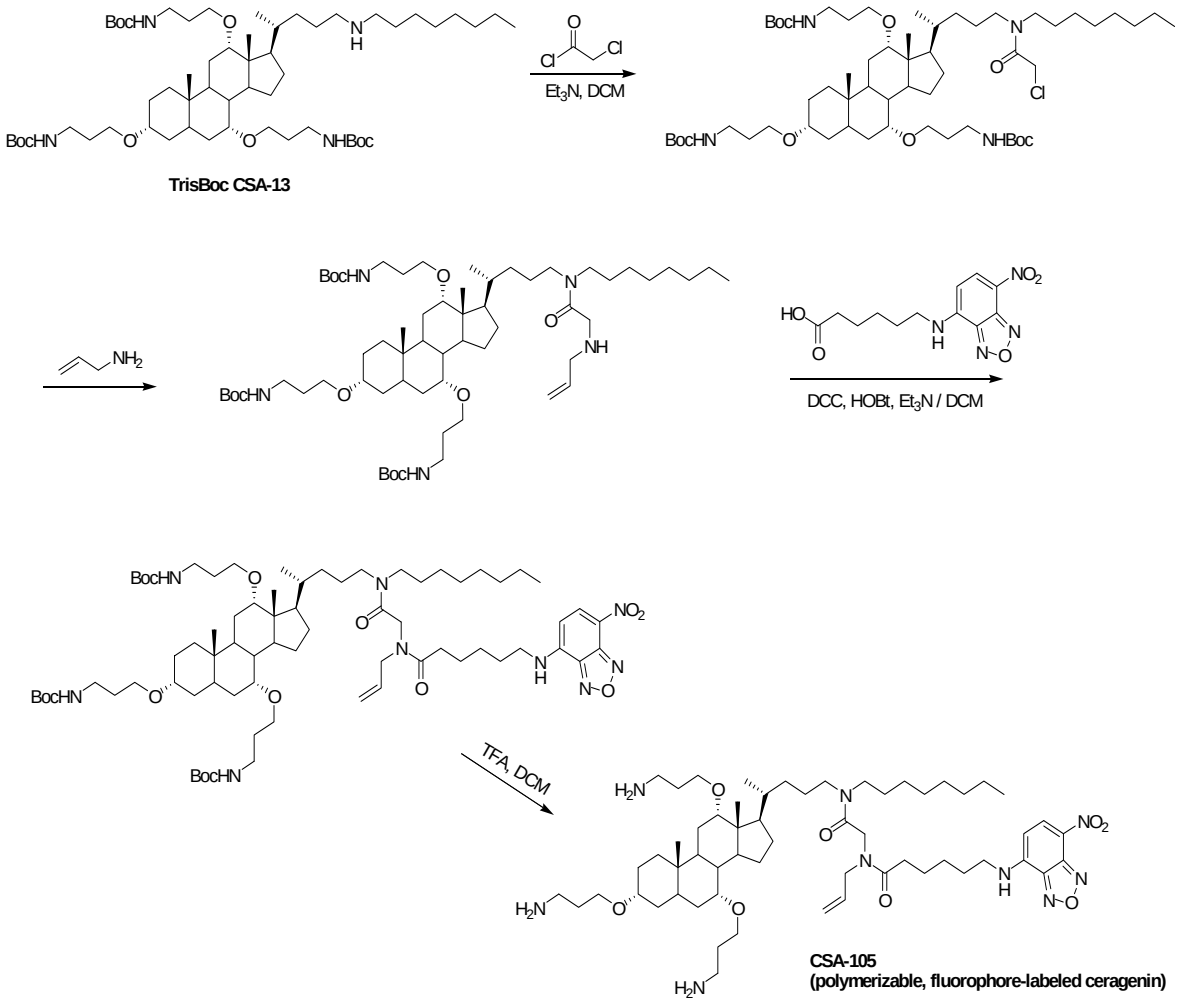

Figure 2. Synthetic scheme for CSA-105.

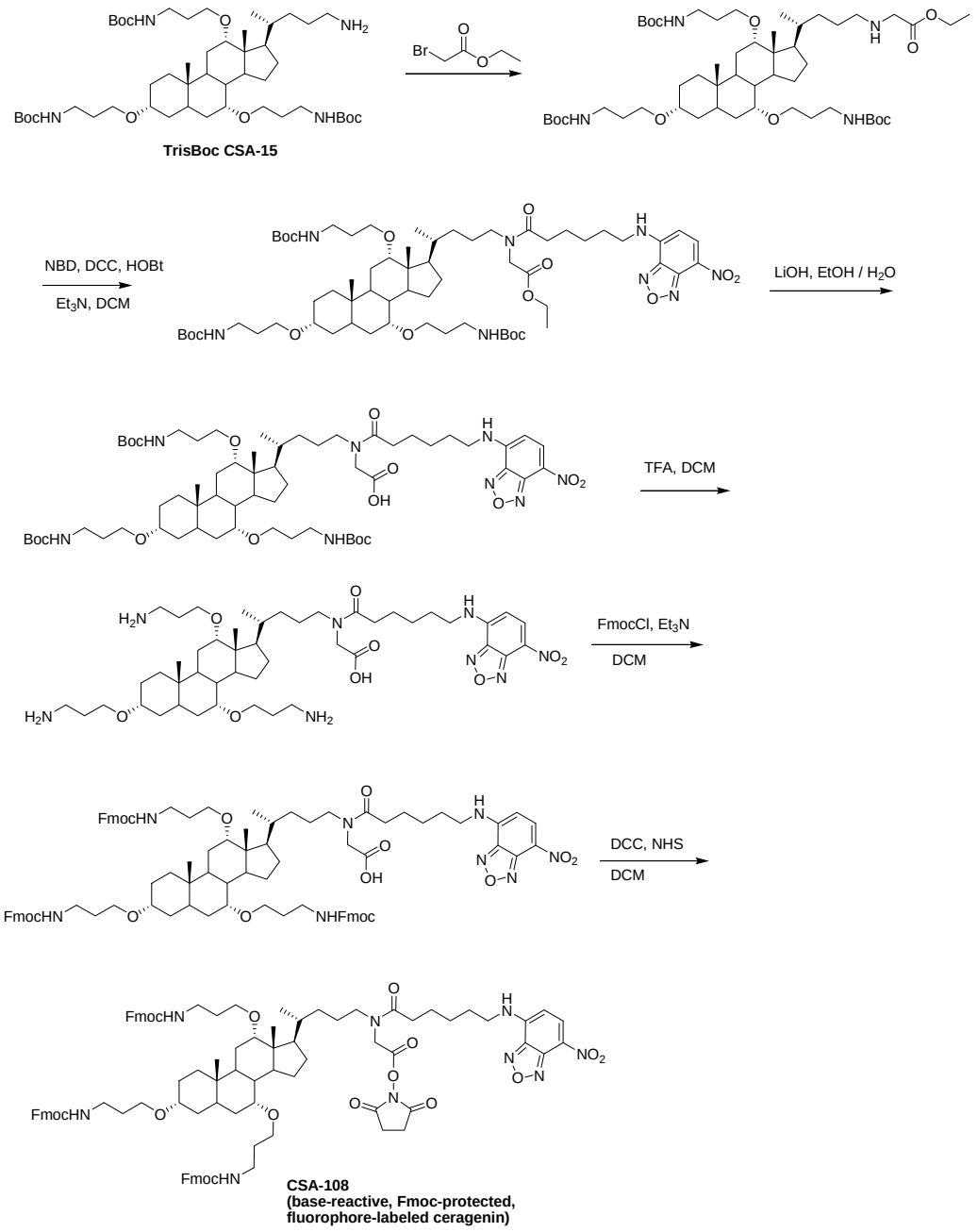

Figure 3. Synthetic scheme for CSA-108.

surface of reverse osmosis (RO) membranes by a radical reaction in which the membrane was immersed in a solution of monomers and initiating agent. The RO membranes used were GE Seta^{TM} brackishwater desalination polyamide membranes purchased from GEOsmonics (part number 1221916 or 1206368). In that report it is unclear what the point of attachment on the membrane surface is since the surface is a crosslinked poly(amide). However the attachment of poly(acrylate)-type oligomers was verified after extensive washing with water. In method 1 (Figure 4), a mixture of CSA-105 and acrylic acid in water was placed on the surfaces of six RO membranes, each bounded by a PTFE o-ring. A solution of initiator was added to each and the

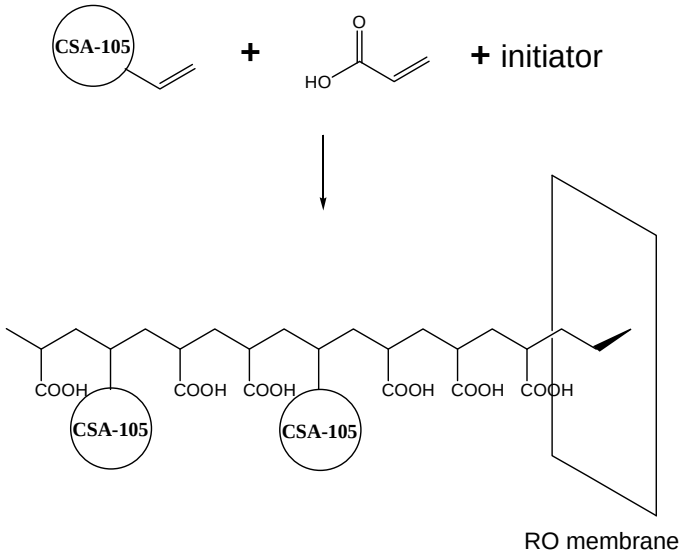

Figure 4. Attachment method 1.

o-rings were then covered to limit evaporation. The reactions were allowed to take place at room temperature and pairs of samples were removed and rinsed thoroughly with water after time intervals of 1, 2, and 24 hours. This method has the advantage that each of the oligomers formed should contain multiple ceragenins, so even if the number of attached oligomers is low, the density of ceragenins could be high.

Method 2 is based on previous work by the Savage group [*Ding et al.*, 2004] in which a ceregenin with a primary amine reacted with an activated ester to form an amide linkage with the ceragenin. For method 2 (Figure 5), the ceragenin (CSA-108) has an activated ester (an N-hydroxysuccinimide group) will readily react with a free amine on the surface of the RO membrane to form an amide linkage. This method is the simplest, most direct way of attaching ceragenins to membranes but it will only allow for one ceragenin to attach per free amine on the surface. Since the concentration of free amines on RO membranes is not well determined, it remains to be seen if this method will impart enough biocidal character to the membranes to

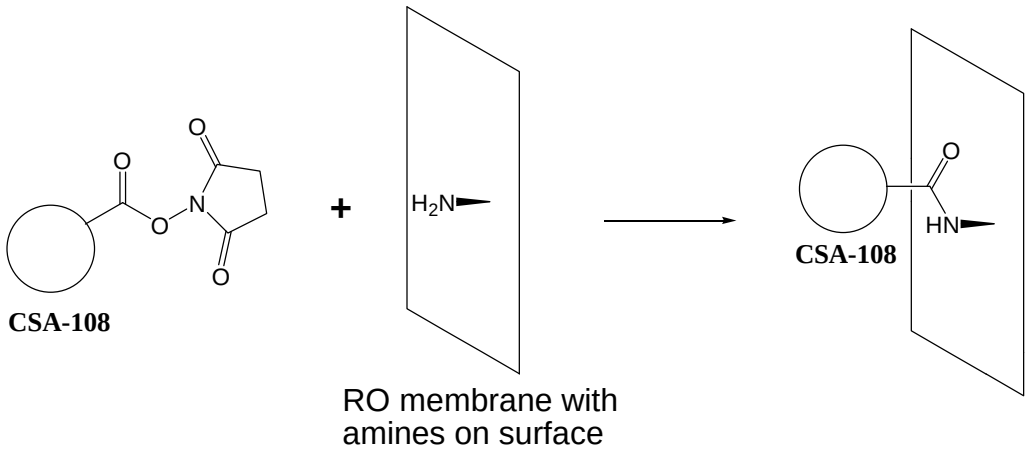

Figure 5. Attachment method 2.

deter biofouling. Additionally, the lack of mobility of the attached ceragenins might reduce their efficacy. If this is determined to be a problem, future experiments will explore the use of oligomeric poly(ethylene glycol)-based tethers to attach the ceragenin

2.2.2 Imaging of Treated Membrane

2.2.2.1 Background and Methods

Hyperspectral imaging was used to characterize and quantify the amount of ceragenin attached to the RO membranes. Hyperspectral imaging when combined with Multivariate Curve Resolution (MCR) is a powerful imaging technique for attaining quantitative information from fluorescence hyperspectral images [*Haaland et al.*, 2007; *Martinez et al.*, 2003; *Nieman et al.*, 2006; *Sutherland et al.*, 2007; *Timlin et al.*, 2005]. Overlapping fluorophores are problematic for many traditional fluorescence microscopy techniques, however hyperspectral imaging with MCR analysis allows us to separate many overlapping fluorophores and create interpretable quantitative images for both known and unknown biological samples. MCR can provide a relative quantitative analysis of the hyperspectral image data without the need for standards, and it discovers all the emitting species present in an image, even those in which we have no *a priori* information.

For this project, we employed two hyperspectral imagers designed and built at Sandia National Laboratories. The first imager, the hyperspectral scanner, was originally built to scan and quantify multiple fluorophores on DNA microarray slides, however this imager is also useful for many applications in which large areas need to be scanned and imaged [*Sinclair et al.*, 2004]. This hyperspectral scanner was used to image large areas of the RO membranes and quantify the amount ceragenin attached to the membrane surface.

For this study, the hyperspectral scanner was used to evaluate ceragenins attachment. A 60 mm^2 area of the dry membranes was imaged using a 488 nm excitation laser and the resultant fluorescence emission was collected onto an electron multiplying charged-coupled device (EMCCD) detector. An infinity-corrected 10× apochromatic objective was used attaining a final pixel size of 30 μm × 30 μm. At this resolution, each image consisted of 66,000 pixels with each pixel having an emission spectrum composed of 532 wavelengths, from 490 to 890 nm, and a spectral resolution of 3 nm. After the collection of the image data, these data were preprocessed to remove cosmic spikes that may have been inadvertently collected onto the EMCCD and to remove image curvature and keystone that are distortions imparted onto the spectral data from the spectrometer. MCR was then used to determine the pure spectral emission components and the corresponding concentration images of the preprocessed spectral images. This imager was used to 1) attain the spectral components of an untreated RO membrane and 2) determine the spatial distribution of ceragenin intensity and median intensity for the treated RO membranes.

The other imager is a 3D confocal hyperspectral fluorescent microscope that was developed to enhance our research into a variety of biological systems at a microscopic level (e.g., host-pathogen interactions in innate immune cells, investigating photosynthesis in cyanobacteria, and understanding plant tissue systems for biofuel applications) [*Sinclair et al.*, 2006]. To image the ceragenins, small amounts of each ceragenin formulation were dissolved in water. Once dissolved, each aqueous solution was placed onto an individual quartz coverslip and allowed to

dry. Each dried formulation was then imaged using a 488 nm excitation wavelength with an infinity-corrected 10x apochromatic objective to collect a 100 μm field of view (FOV) image. Only one confocal slice was collected for each X-Y location. At this FOV, each pixel was 0.5 by 0.5 μm in size and each image consisted of 204 by 208 pixels for a total of 42432 pixels or spectra. Each emission spectrum consisted of 512 wavelengths with a spectral resolution of 1-3 μm. Prior to the MCR analysis of these hyperspectral images, these images were preprocessed to improve the quality of the spectral data. The preprocessing steps included: 1) removing cosmic spikes that may have been inadvertently collected onto the EMCCD 2) subtracting the dark image from the data and 3) removing an offset component that is added to the spectral data during the image collection step. After the hyperspectral image data were preprocessed, MCR was used to extract the pure emission spectra along with the corresponding concentration (intensity) images for each pure spectrum. These concentration images were then used to create RGB images for the various ceragenin formulations to check for homogeneity of the emission components. This imager was used to 1) attain spectral components of CSA-13, CSA-105, and CSA-109 and 2) examine CSA-105 in more detail to understand the ceragenins homogeneity.

2.2.2.2 Results

To identify the individual spectral components hyperspectral images were collected on 1) an untreated RO membrane, and 2) CSA-13, CSA-105, and CSA-109 individually. The untreated membrane was imaged using the hyperspectral scanner, while three different dried ceragenin formulations (CSA-13, CSA-105, and CSA-109) were imaged using the 3D confocal hyperspectral microscope. MCR analyses extracted the pure emission spectra from the hyperspectral images for the RO membrane and the three different ceragenin formulations (Figure 6). Due to spectral artifacts, each real spectral component had a spectral shift component associated with it. On the hyperspectral scanner, these spectral shift components are related to the imperfect correction of the keystone and curvature artifacts associated with the imager. On the 3D confocal microscope, these spectral shift components are thought to be due to changes in the refractive indices of these dried samples. Due to these spectral shift components, the peak locations listed below are approximate and could change depending on how MCR models the shift and real components of the images (the MCR model is a linear combination of the real and shift components).

The RO membrane has two distinct autofluorescent components with peaks at approximately 522 and 595 nm (Figure 6A). The second autofluorescent component (Autofluorescence #2) is weak and cannot be detected when much stronger fluorophores are present. The CSA-13 (ceragenin without an amide connector or a fluorophore) has an autofluorescence component with a peak at approximately 554 nm; however, it is extremely weak (Figure 6B). Unexpectedly, CSA-109 (ceragenin with an amide connector but no fluorophore) had a distinct autofluorescent component with a peak at approximately 600 nm (Figure 6C). This result might suggest that the amide connector has its own distinct autofluorescent component. Finally, the spectral components detected when imaging CSA-105 (ceragenin with an amide connector and NBD fluorophore) include the component detected when imaging CSA-109 and the component expected from the NBD (Figure 6D). In summary, we determined that while the ceragenin has its own autofluorescence, it is relatively weak compared to that of the untreated RO membrane, the amide connector and the NBD fluorophore. In addition, the CSA-105 has two distinct

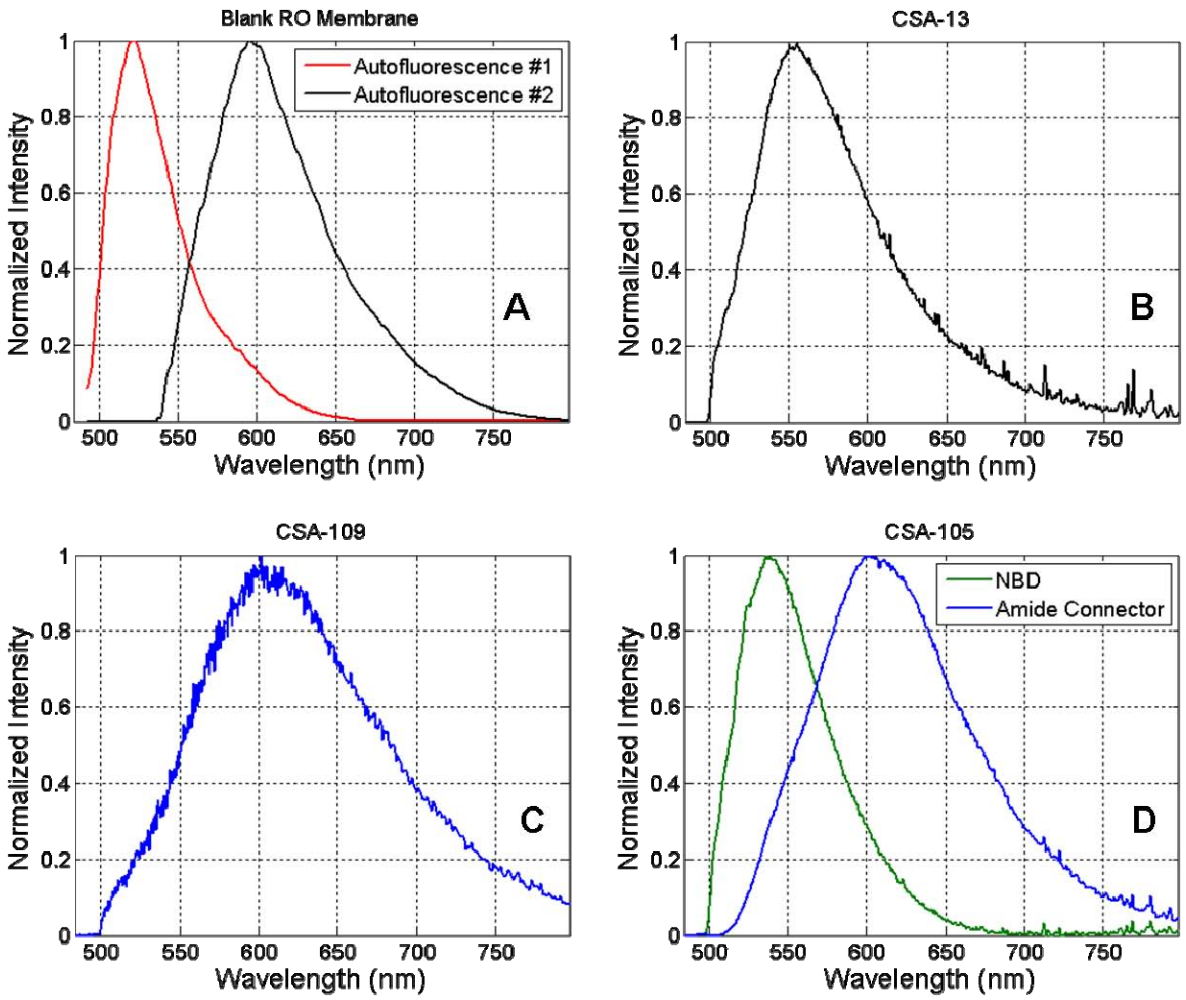

Figure 6. Pure spectral components of (A) an untreated RO membrane, (B) CSA-13, (C) CSA-109, and (D) CSA-105. Current results suggest that membrane Autofluorescence #2 (A) and autofluorescence in CSA-13 (B) are weak and should be hard to detect in the presence of any other stronger emitting fluorophores.

components, one from the amide connector and the other from the NBD fluorophore. Unfortuntately, there appears to be overlap between these two components and that detected in the autofluorescence of the untreated RO membrane.

Although a comparison between the intensities of the various formulations and the RO membrane are made above, there was no attempt to keep the concentrations of the formulations constant. Future experiments should consist of imaging these ceragenin solutions at the same concentration to get a better understanding of the relative emission intensities of the various formulations. With a complete understanding of the relative emission intensities and the noise characteristics of our imagers, an evaluation of the sensitivity of our measurement can be determined.

Three membranes coated with ceragenin (CSA-105 – ceragenin with an amide connector and NBD fluorophore) as described Section 2.1.2 and 2.2.1 were imaged using the hyperspectral

scanner [*Sinclair et al.*, 2004]. The three pure spectral components obtained from MCR for the ceragenin coated membranes (Figure 7) are: 1) the stronger of the two components from the autofluorescence of the membrane shown in Figure 6A, 2) the NBD fluorophore as seen in Figure 6D, and the amide connector component as seen in Figure 6C and D.

Figure 8 presents both concentration images and the corresponding intensities for both the NBD fluorophore and the amide connector spectral components from Figure 7. The median intensity of both the NBD fluorophore and the amide connector autofluorescence increases as a function of the reaction time of the RO membrane with the ceragenin solution. It also appears that the 24 hour reaction time provides the best spatial ceragenin coverage across the membrane. Although, the images look more uniform at 24 hours, there still appears to be very bright anomalies present.

The 3D confocal hyperspectral microscope was used to investigate these anomalies. There appears to be large particulates of excess NBD in the ceragenin that did not attach to the ceragenins core via the amide connector (Figure 9).

The initial plan was to use the NBD fluorophore to visualize the ceragenin coating on the membrane. However since this amide connector is necessary to connect the ceragenin to the membrane and it has fluorescence, we may not need an explicit fluorophore to be attached to the ceragenin to characterize the coating quality. We will use hyperspectral imaging in future studies to develop a membrane coating protocol that provides the best coating coverage and uniformity for our RO membranes.

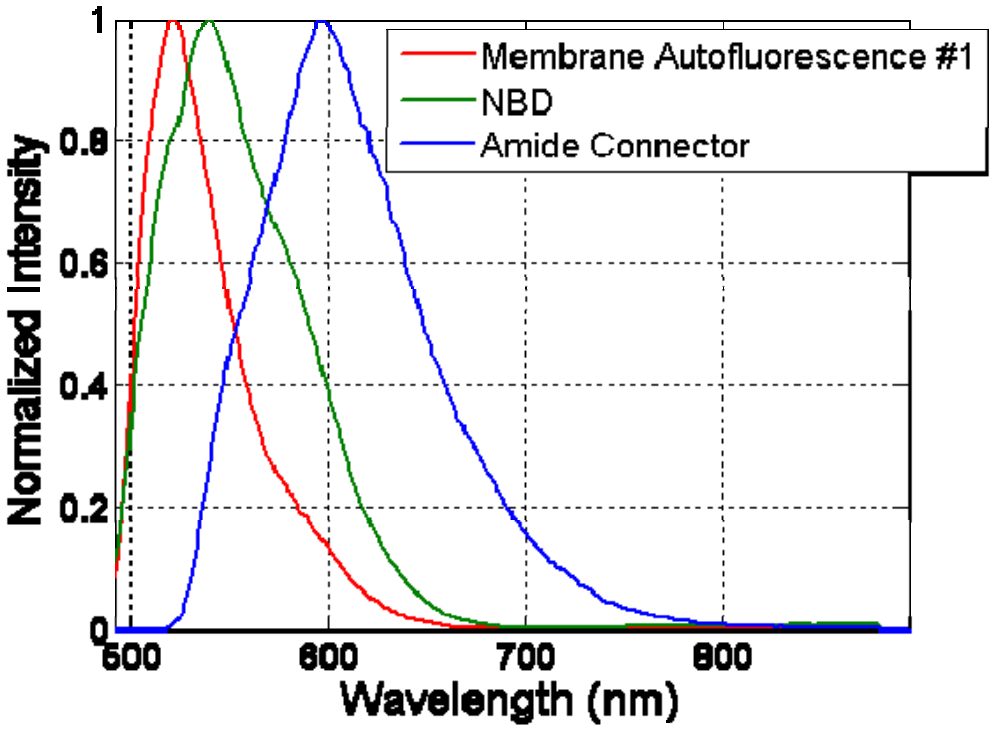

Figure 7. Pure spectral components of ceragenin (CSA-105) treated RO membrane. The red spectrum is the native auto-fluorescence present in the RO membrane, the green spectrum is the NBD fluorophore attached to the ceragenin and the blue spectrum is due to the amide connector.

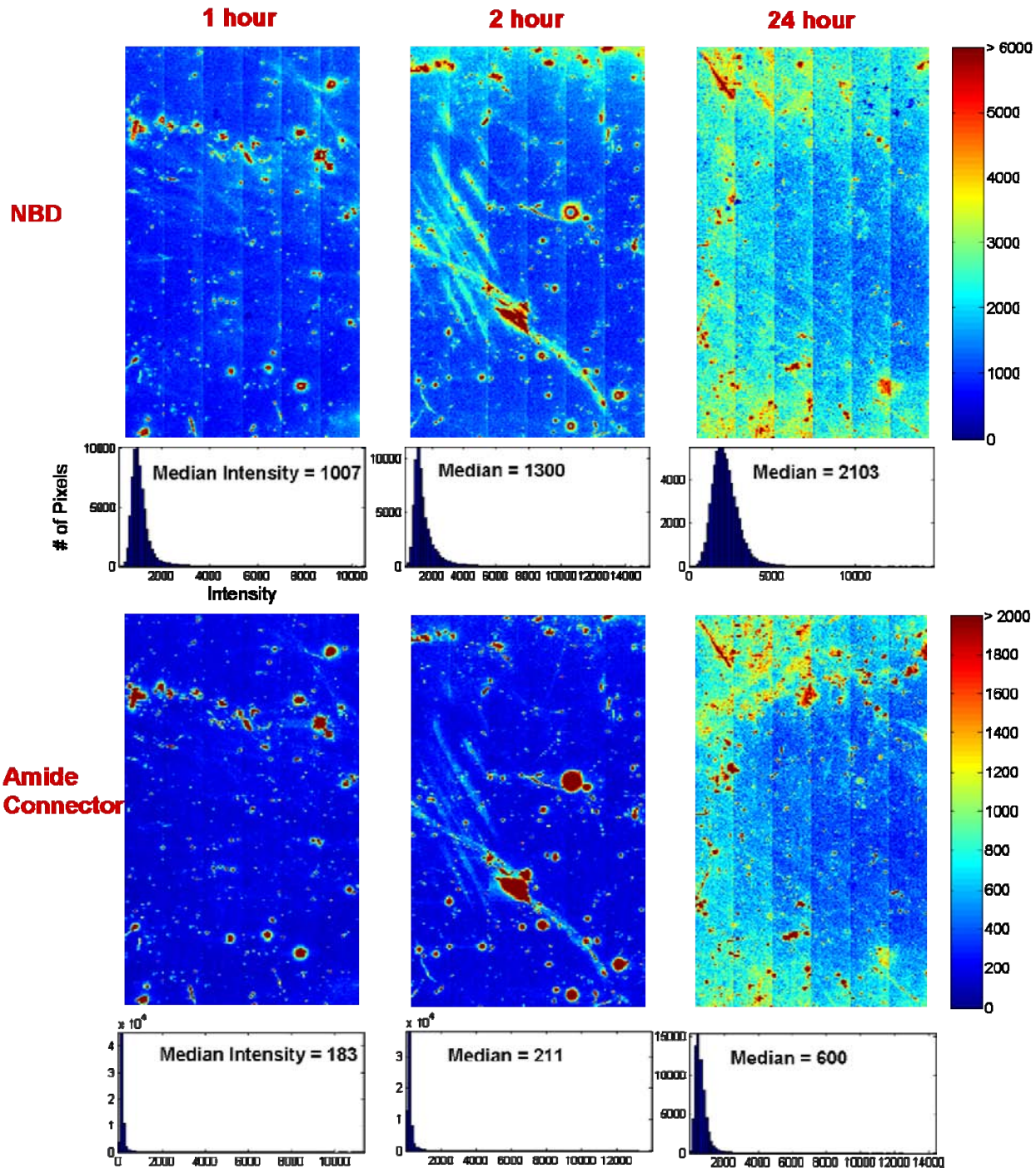

Figure 8. Concentration images of the NBD fluorophore and the amide connector autofluorescence components found in the CSA-105 treated membranes. These concentration images have been altered to improve the contrast (intensities at or above 6000 for the NBD component or 2000 for the amide connector component are represented with the same color). Histograms for each concentration map are shown beneath each image, where a bar represents the number of pixels (y-axis) at a specific concentration or intensity (x-axis). The median concentration of both components increases as function of reaction time. It also, appears that the coating becomes more uniform after 24 hours of reaction time. Dimensions of these images acquired on the hyperspectral scanner are 6 x 10 mm in size with the pixel size being 30 μm square.

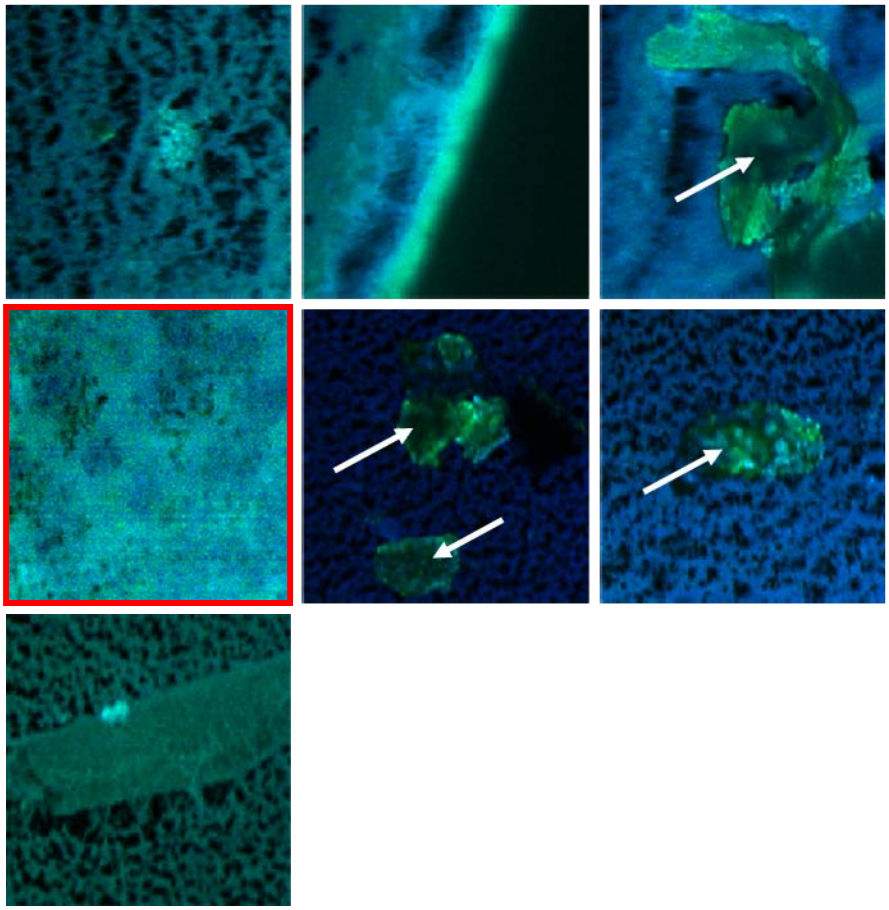

Figure 9. Pure images of ceragenin (CSA-105) taken with confocal imager. The NBD fluorophore is shown in green and the amide connector autofluorescence component is shown in blue (see Figure 6 for spectra). Images have a 100-μm field of view with a pixel size of 0.5 μm square. Just like the ceragenin (CSA-105) coated membranes, these images have what appears to be NBD particulate that is not bound to the amide connector (as indicated by the white arrows). The image outlined in red shows the highest degree of uniformity.

3 BIOCIDAL ACTIVITY OF CERAGENINS

This section presents minimum inhibition concentration and minimum bactericidal concentration of *Pseudomonas fluorescens* with CSA-13. Testing of the biocidal activity of CSA-13 on a *Pseudomonas fluorescens* biofilm is presented. Finally, testing of the biocidal activity of CSA-105 attached to a water-treatment membrane is also discussed.

3.1 MICs and MBCs

Minimum inhibition concentration (MICs) and minimum bactericidal concentrations (MBCs) are typically used to assess antibacterial activity on planktonic bacteria. MICs measure at what concentration a compound, in this case the ceragenin, inhibits the growth of a bacteria strain. MBCs measure at what concentration a compound kills the bacteria. MICs and MBCs have been reported for CSA-13 against *Pseudomonas aeruginosa* [*Chin et al.*, 2008], CSA-8 and CSA-13 for *Staphylococcus aureus* [*Chin et al.*, 2007], and CSA-13 compared to other antibiotics against many clinical isolates of drug-resistant *S. aureus* [*Lai et al.*, In Press]. *Pseudomonas fluorescens* is the bacteria being used to evaluate the ceragenins on RO membranes, therefore, MICs and MBCs for CSA-13 on *P. fluorescens* was deemed important.

3.1.1 Methods

Kill kinetics were performed with CSA-13 for *P. fluorescens* [ATCC 700830] using the protocol in *NCCLS* [1997]. The assay was performed in Mueller-Hinton broth (MHB) at time points 2, 4 and 6 hours on a 10^6 CFU/mL inoculate of *P. fluorescens*. Assays were performed in triplicate. A 100 µL sample was removed at each time point, serially diluted, plated on Mueller-Hinton agar (MHA), and incubated at 37^o C for 24 hours. Triplicate plates were generated for each sample. Plates were counted and kill kinetics were determined. MIC was determined by comparing the data collected after 2 hours of incubation to the initial inoculum concentrations. If the concentration decreased, then that ceragenin concentration is considered to be at or above the MIC. MBC was determined by the concentration at which 100% of the initial inoculum was killed. The CSA-13 concentrations examined were 1, 2, 3, 4 and 5 µg/mL.

3.1.2 Results

Results indicate a MIC of approximately 1 µg/L of CSA-13 for *P. fluorescens* (Figure 10). This can be seen by the greater than four log reduction in *P. fluorescens* concentrations after 2 hours of incubation. Given the large decrease, it is possible that the MIC could be even lower than 1 µg/L of CSA-13. The MBC was approximately 2 µg/L (Figure 10) as seen by the 100% kill rate with CSA-13 concentrations of 2 µg/L for incubation times of 4 hours and greater.

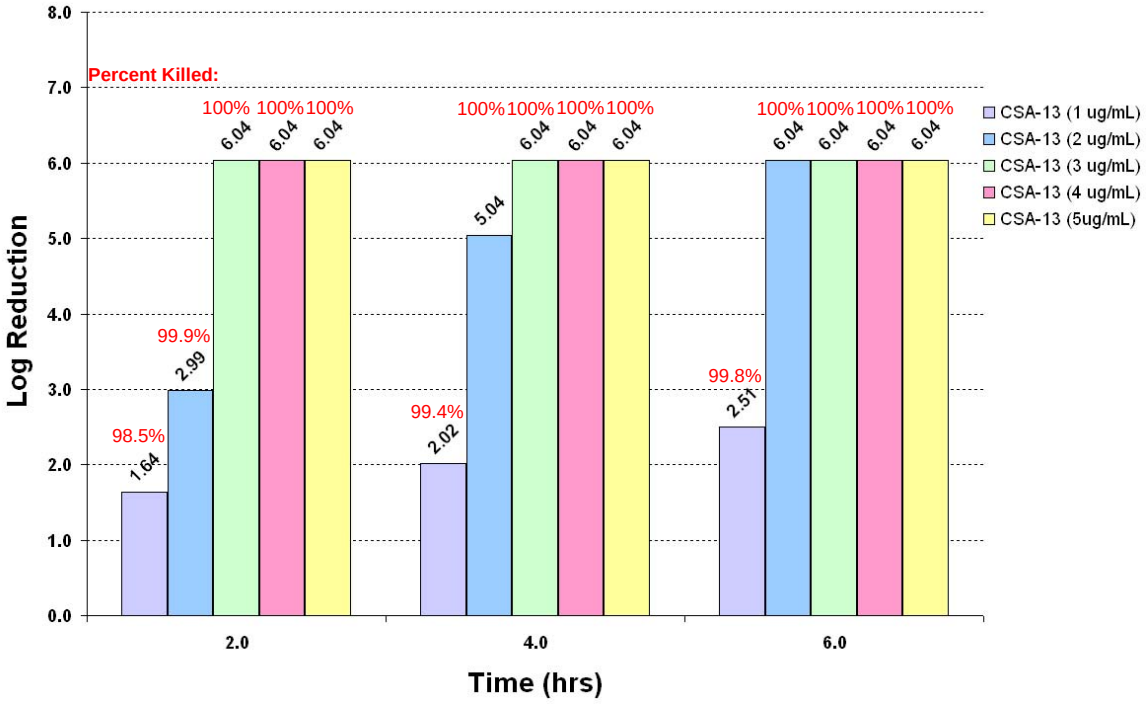

Figure 10. Results showing a MBC of approximately 2 µg/mL of CSA-13 with *Pseudomonas fluorescens*. Percent killed values are shown in red.

3.2 Impact of ceragenins on established biofilms

The purpose of this experiment was to determine if ceragenins were effective in killing bacteria in established biofilms. To do this, biofilms were grown in a drip flow reactor. After biofilm development, a solution containing ceragenins was pipetted on to the biofilm. The biofilm was then stained with a live/dead stain and examined microscopically to determine whether it differed from a biofilm that had not been treated with ceragenins.

3.2.1 Methods

Biofilms were grown in a drip flow reactor using glass microscope slides. Each of four chambers of the reactor were filled with 1 ml of 2.3×10^9 CFU/ml of *Pseudomonas fluorescens* [ATCC 700830] inoculum and 10 ml of pure Trypticase Soy Broth (TSB). The *P. fluorescens* incubated in the reactor in the flat position for 24 hours. After this incubation period, the reactor was tilted so the slope was approximately 10˚ and dripping of nutrient and neutralizing solutions commenced at a flow rate of 1 ml/min. Solutions of 1:100 TSB were used. Flow through the chambers continued for 6 days.

After growing the biofilms, two slides had 10 µl of 139 µg/ml of the CSA-13 dropped in the middle of the slide. The other two samples were untreated. The slides were allowed to sit for 10 minutes prior to staining. The biofilms were stained with LIVE/DEAD® *Bac*Light™ bacterial viability kit (Invitrogen) using 30 µM propidium iodine and 5 µM SYTO® 9. The stain remained on the biofilm for 15 minutes in the dark before it was rinsed three times with 0.1 M $NaHCO_3$.

Propidium iodine, which fluoresces red in the visible spectral region, only penetrates cell membranes that are compromised and is thus indicative of dead or compromised cells. SYTO® 9, which fluoresces green in the visible spectral region, indicates live cells or cells with uncompromised cell membranes.

The 3D hyperspectral confocal microscope was used to measure the effect of applying ceragenin to the surface of the biofilm. Images were acquired with a 20x objective (50 µm FOV) using 488 nm laser excitation. Nine confocal optical sections were acquired penetrating to a total depth of 8 µm into each biofilm sample imaged. Images were acquired on both the samples with and without ceragenin applied to the biofilm. Once these images were acquired, MCR was used to generate the pure component spectra of SYTO® 9 and propidium iodide, as well as the corresponding concentration (intensity) images for each component. Also, the concentration images of SYTO® 9 were divided by the concentration images of propidium iodide to provide images of the live/dead ratios of the bacteria in the images.

3.2.2 Results

Data collected from the hyperspectral imager indicate that there are more dead or compromised cells in the biofilm that was treated with the ceragenins. Figure 11 shows two representative optical sections (one with no ceragenins added and one with ceragenins added). There are two

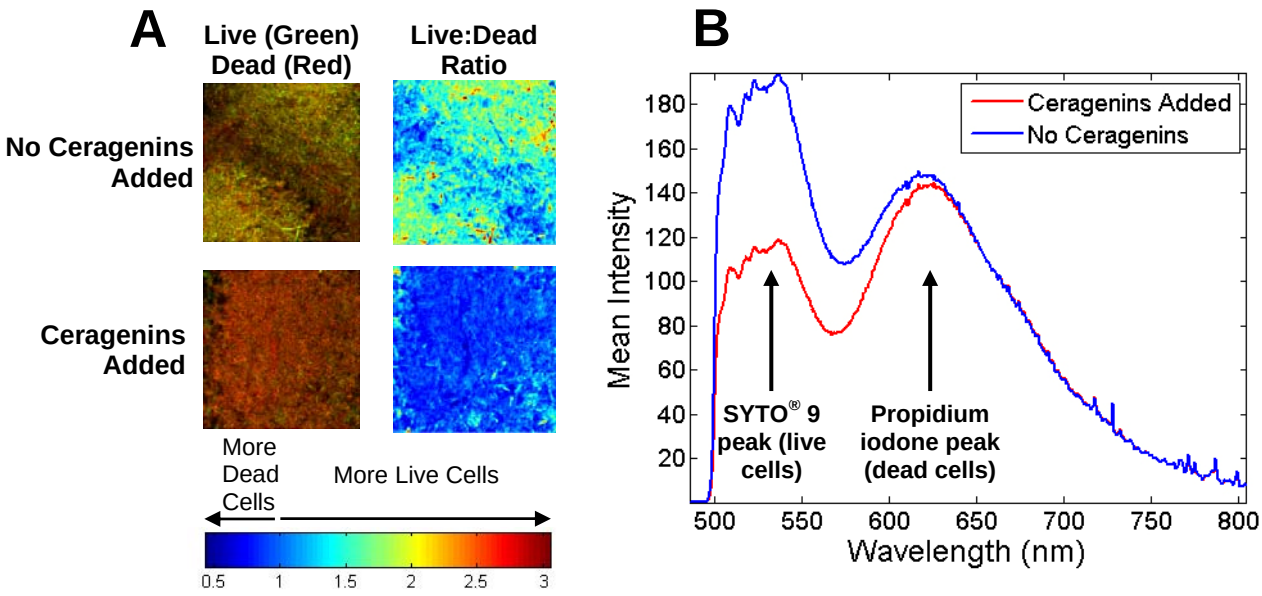

Figure 11. Hyperspectral data showing more dead cells in ceragenin-treated biofilms. Images (A) showing LIVE/DEAD® staining with more cells stained with propidium iodine (red) in the ceragenin-treated biofilm and more compromised cells when looking at the Live:Dead ratio. Plot of mean intensity of all the voxels in the entire image (B) showing greater SYTO® 9 intensity for the untreated sample (blue line) indicating more live cells and greater propidium iodine intensity for ceragenin-treated biofilm (red line), indicating more compromised cells.

sets of images in Figure 11. The first set of images is RGB images in which SYTO® 9 is represented in green and propidium iodide is represented in red. The ceragenins–treated sample appears more red and the untreated sample appears more green indicating that the bacteria appear to more compromised when treated with ceragenin. This is further confirmed when looking at the second set of images. These live/dead (SYTO® 9/propidium iodide) ratio images show that there are more dead bacteria in the sample when ceragenins had been added. Another way to use the spectral image data is to look at the mean spectrum obtained from the approximately 40,000 spectra in each image and directly compare the peak intensities of SYTO® 9 with the peak intensities of propidium iodide. Figure 11 shows the peak intensity of propidium iodide (more dead bacteria) is greater than the peak intensity of SYTO® 9 for the image where ceragenins were added to the biofilm. The opposite is true when there was no ceragenin added to the biofilm.

3.3 Testing of membranes with attached ceragenins

After successfully attaching the ceragenins to the RO membranes (see Section 2.2.2). These membranes were exposed to bacteria for the purposes of imaging on the confocal hyperspectral microscope and enumeration (via plate counts) to determine the biocidal activity of the attached ceragenin. Unfortunately, the proper staining protocol was not followed when preparing the samples for the hyperspectral imager. Therefore, only the results from the enumeration experiment are reported here, however methods outlining the sample preparation for both imaging and enumeration have documented in the methods section.

3.3.1 Methods

Two sample preparation protocols were used for testing the biocidal activity of the ceragenins on RO membranes. For imaging, six membranes were put into centrifuge vials with a solution of bacteria. For enumeration experiment, only the side of the membrane that was treated with ceragenins could be exposed to bacteria, so a second protocol was developed. In both tests, six membranes were analyzed: three with ceragenins attached and three untreated RO membranes. The ceragenin-coated membranes had reaction times of 1, 2, and 24 hours as described in section 2.2.2.

3.3.1.1 Imaging Test

Prior to the start of the tests, the six membranes were disinfected by soaking them in ethanol overnight. 20 ml of 6.2×10^5 CFU/ml of *Pseudomonas fluorescens* [ATCC 700830] inoculum was added to a sterile 50 ml conical centrifuge vials (Falcon 21088-939). Each membrane was removed from the ethanol and rinsed with copius amounts of sterile deionized water and placed into a labeled vial. The vials were allowed to incubate on a shaker table set at 50 rpm for 24 hours. The solutions were then sampled from each vial for plating. The remaining liquid was poured out of the tube and the membrane removed. The membrane was rinsed three times with sterile deinoize water and then stained with the LIVE/DEAD® BacLight™ as described in Section 3.2.1. Unfortunately, the stain was never rinsed off prior to imaging, which adversely affected the imaging results.

3.3.1.2 Enumeration Test

Glass vacuum filter holders [Advantec 13 mm Glass Microanalysis Holders] as shown in Figure 12 were used for the plate counting tests. The filter holders were autoclaved at 121 ˚C and 15 psi for 15 minutes prior to the start of the experiment. To maintain sterility, both the top and bottom were covered with aluminum foil prior to autoclaving. A small amount of silicon grease was also applied to one side of the filter holder. The grease was needed to prevent leaking during the test. Likewise, the RO membranes were sterilized by soaking in ethanol overnight. Each membrane was placed in the glass filter holder and this apparatus placed on a shaker table. 5 ml of 6.2×10^5 CFU/ml of *Pseudomonas fluorescens* inoculum was added to the top of the filter holders. The systems were allowed to shake at 50 RPM while at room temperature for approximately 24 hours.

Following the 24 hours, the membranes were then ready for sampling. Each membrane was removed from the bottom part of the filter holder with sterile tweezers and rinsed 3 times with the sterile DI water. The membrane was placed into a 15 ml conical vial (VWR 20171-008) filled with 10 ml of sterile DI water. The vial was vortexed, sonicate for 15 minutes, and then vortex again. An 1 ml aliquot of this solution was then plated for enumeration.

Samples for plating were serially diluted and enumerated using Trypticase Soy Agar (TSA). Triphenyl Tetrazolium Chloride (BD Biosciences) was added to the TSA to facilitate enumeration. The volume concentration of Triphenyl Tetrazolium Chloride was 0.01%. Quadruplicate plates were prepared for each dilution. Plates were incubated at 30 °C for 48 hours prior to enumerating. Results are reported as the mean and standard deviation of the four plates.

3.3.2 Results

Results of the enumeration test indicate that the amount of bacteria on ceragenin-coated membrane that reacted with the ceragenin solution for 1 hour is not significantly different than

Figure 12. Photograph of glass filter holders used to test biocidal activity on ceragenin-treated RO membranes.

the controls (Table 1 and Figure 13). However, the cell density on the membrane that reacted with the ceragenin solution for 24 hours was approximately 1 order of magnitude less than the control (Table 1 and Figure 13). These preliminary results are not as strong as testing conducted on endotracheal tubes where counts remained less than 50 CFU's after 14 days of soaking in bacterial solution (Paul Savage, personal communication). However, for a first try, these results are still promising.

Table 1. Results of Enumeration Tests

Sample Description	Average (Standard Deviation) Bacteria Density on Membrane (CFU/cm^2)	Average (Standard Deviation) Final Bacteria Concentration in Solution (CFU/ml)
Control 1	Membrane Contaminated	7.2×10^7 (5.7×10^6)
Control 2	2.1×10^7 (1.9×10^6)	7.5×10^7 (7.4×10^6)
Control 3	7.6×10^6 (1.1×10^6)	4.9×10^8 (7.0×10^7)
1-hr ceragenin coating time	1.1×10^7 (1.1×10^5)	8.3×10^8 (6.1×10^7)
2 hr ceragenin coating time	Membrane Contaminated	7.3×10^8 (1.1×10^8)
24-hr ceragenin coating time	9.6×10^5 (6.6×10^4)	2.6×10^8 (4.8×10^7)

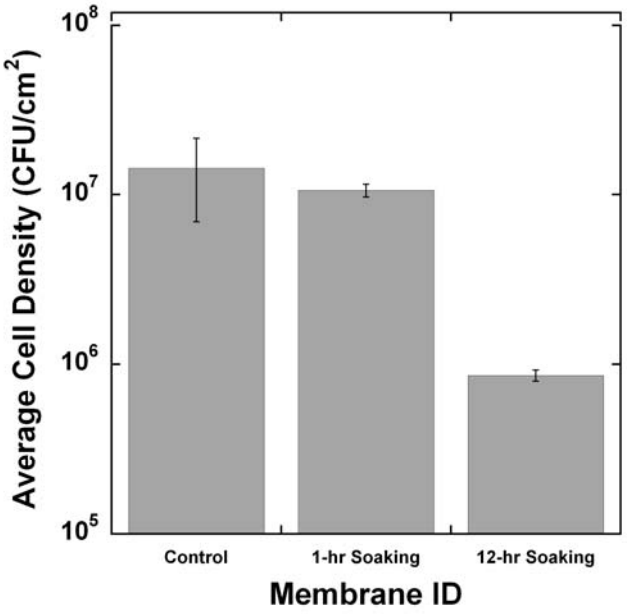

Figure 13: Results of enumeration testing showing that membrane soaked in ceragenin solution for 24 hours yielded cell densities approximately an order of magnitude lower than the controls and the membrane that soaked in the ceragenin solution for 1 hour.

4 SUMMARY AND FUTURE WORK

The work presented in this report provides evidence that

- The ceragenins CSA-105 can be attached to RO membranes
- The ceragenin CSA-13 is effective at killing planktonic *Pseudomonas fluorescens* with measured MIC's of approximately 1 μg/L and MBC of 2 1 μg/L.
- The ceragenin CSA-13 is effective at killing *Pseudomonas fluorescens* in biofilms

In addition, there is promising evidence that less viable *P. fluorescens* will stick to a RO membrane with linked ceragenins than to an untreated membrane as shown in Figure 13.

This study allowed for a careful analysis of our techniques for imaging ceragenins. It was discovered that there were three fluorescent components present when imaging the ceragenin membranes: a component that is related to the autofluorescence from membrane, the NBD fluorophore, and a component somehow related to the amide connector that is attached to the ceragenin. NBD was also an effective fluorescent tag. However, the spectrum of the NBD had much greater overlap with that of the autofluorescence of the untreated RO membrane. Future work will include better assessing the relative intensities of the different fluorescent components to determine whether the fluorescence signal emanating from the amide connector is sufficient for characterizing the ceragenin coating or whether an explicit fluorophore is needed. In addition, artifacts due to spectral shift components in the hyperspectral imagers need to be better understood in order to determine more accurate peak locations and spectral components.

Images of RO membranes treated with CSA-105 indicated inhomogeneous attachment of the ceragenin to the membrane. Additional work is needed to more uniformly attach the ceragenin. This will be done by developing a two-step procedure for attachment method 1. The first step will be to treat the membrane surface with an epoxy-alkene such as 3,4-epoxy-1-butene in order to allow the amines on the surface to react with the epoxy groups. After washing off the excess epoxy-alkene, the surface will have covalently bound alkene groups which will serve as the points of attachment for the poly(acrylate)-type oligomers which will be formed in the second step as described in section 2.2.1 above. This method will also eliminate the ambiguity in the attachment mechanism. In addition to this change in the procedure for method 1, a better apparatus for bounding the reaction solution on the membrane surface has been developed. Instead of using an o-ring, a polycarbonate frame will be compressed against the membrane surface to hold the solution in place. It will be deep enough to allow for an even depth of reaction solution over the entire surface and it will be covered to prevent solvent evaporation during the attachment procedure.

In summary, this scoping study has provided promising evidence that linking ceragenins to water-treatment membranes could create biofouling resistant water-treatment membranes. However, future work is needed in order to better design the membrane and completely test the biocidal effectiveness of the ceragenin in this context.

5 REFERENCES

Belfer, S., Y. Purinson, R. Fainshtein, Y. Radchenko, and O. Kedem (1998), Surface modification of commercial composite polyamide reverse osmosis membranes, *J. Membr. Sci.*, *139*, 175-181.

Chin, J. N., R. N. Jones, H. S. Sader, P. B. Savage, and M. J. Rybak (2008), Potential synergy activity of the novel ceragenin, csa-13, against clinical isolates of pseudomonas aeruginosa, including multidrug-resistant p. Aeruginosa, *Journal of Antimicrobial Chemotherapy*, *61*, 365-370.

Chin, J. N., M. J. Rybak, C. M. Cheung, and P. B. Savage (2007), Antimicrobial activities of ceragenins against clinical isolates of resistant staphylococcus aureus, *Antimicrobial Agents and Chemotherapy*, *51*, 1268-1273.

Ding, B. W., N. Yin, Y. Liu, J. Cardenas-Garcia, R. Evanson, T. Cirsak, M. J. Fan, G. Turin, and P. B. Savage (2004), Origins of cell selectivity of cationic steroid antibiotics, *Journal of the American Chemical Society*, *126*, 13642-13648.

Haaland, D. M., H. D. T. Jones, M. B. Sinclair, B. Carson, C. Branda, J. F. Poschet, R. Rebeil, B. Tian, P. Liu, and A. R. Brasier (2007), Hyperspectral confocal fluorescence imaging of cells - art. No. 676509, paper presented at Conference on Next-Generation Spectroscopic Technologies, Boston, MA, Sep 10-11.

Jenssen, H., P. Hamill, and R. E. W. Hancock (2006), Peptide antimicrobial agents, *Clinical Microbiology Reviews*, *19*, 491-+.

Lai, X.-Z., Y. Feng, J. Pollard, J. N. Chin, M. J. Rybak, R. Bucki, R. F. Epand, R. M. Epand, and P. B. Savage (In Press), Ceragenins: Cholic acid-based mimics of antimicrobial peptides, *Accounts of Chemical Research*.

Martinez, M. J., A. D. Aragon, A. L. Rodriguez, J. M. Weber, J. A. Timlin, M. B. Sinclair, D. M. Haaland, and M. Werner-Washburne (2003), Identification and removal of contaminating fluorescence from commercial and in-house printed DNA microarrays, *Nucleic Acids Research*, *31*.

NCCLS (1997), *Methods for dilution antimicrobial susceptibility tests for bacteria that grow aerobically; approved standard m7-a4*, 4th ed ed., National Committee for Clinical Laboratory Standards, Villanova, PA.

Nieman, L. T., M. B. Sinclair, J. A. Timlin, H. D. T. Jones, and D. M. Haaland (2006), Hyperspectral imaging system for quantitative identification and discrimination of fluorescent labels in the presence of autofluorescence, paper presented at 3rd IEEE International Symposium on Biomedical Imaging, Arlington, VA, Apr 06-09.

Ridgway, H. F., A. Kelly, C. Justice, and B. H. Olson (1983), Microbial fouling of reverse-osmosis membranes used in advanced wastewater-treatment technology - chemical, bacteriological, and ultrastructural analyses, *Appl Environ Microbiol*, *45*, 1066-1084.

Savage, P. B. (2002), Cationic steroid antibiotics, *Current Medicinal Chemistry - Anti-Infective Agents*, *1*, 293-304.

Savage, P. B., C. H. Li, U. Taotafa, B. W. Ding, and Q. Y. Guan (2002), Antibacterial properties of cationic steroid antibiotics, *FEMS Microbiology Letters*, *217*, 1-7.

Sinclair, M. B., D. M. Haaland, J. A. Timlin, and H. D. T. Jones (2006), Hyperspectral confocal microscope, *Applied Optics*, *45*, 6283-6291.

Sinclair, M. B., J. A. Timlin, D. M. Haaland, and M. Werner-Washburne (2004), Design, construction, characterization, and application of a hyperspectral microarray scanner, *Applied Optics*, *43*, 2079-2088.

Sutherland, V. L., J. A. Timlin, L. T. Nieman, J. F. Guzowski, M. K. Chawla, P. F. Worley, B. Roysam, B. L. McNaughton, M. B. Sinclair, and C. A. Barnes (2007), Advanced imaging of multiple mrnas in brain tissue using a custom hyperspectral imager and multivariate curve resolution, *Journal of Neuroscience Methods*, *160*, 144-148.

Timlin, J. A., D. M. Haaland, M. B. Sinclair, A. D. Aragon, M. J. Martinez, and M. Werner-Washburne (2005), Hyperspectral microarray scanning: Impact on the accuracy and reliability of gene expression data, *Bmc Genomics*, *6*.

Vrouwenvelder, H. S., J. A. M. vanPaassen, H. C. Folmer, J. A. M. H. Hofman, M. M. Nederlof, and D. vanderKooij (1998), Biofouling of membranes for drinking water production, *Desalination*, *118*, 157-166.

Watson, I. C., J. Morin, O. J., and L. Henthorne (2003), Desalting handbook for planners, 72, 233 pp, United States Department of the Interior, Bureau of Reclamation, Denver, CO.

DISTRIBUTION

Internal (Hard Copy)

8	MS–0754	S. Altman, 6316
1	MS–0895	H. Jones, 8632
1	MS-0888	M. Hibbs, 6338

Internal (Electronic Copy)

1	MS–0899	Technical Library, 9536
1	MS–0123	LDRD Office
1	MS–0735	J. Merson, 6310
1	MS–0735	R. Finley, 6313
1	MS–0754	P. Brady, 6310
1	MS–0754	R. Cygan, 6316
1	MS-0754	M. Rigali, 6316
1	MS–0754	L. McGrath, 6316
1	MS-0706	D. Borns, 6312
1	MS–0734	B. Kelley, 6327
1	MS-0888	M. Hibbs, 6338
1	MS-0734	J. Tillerson, 6338
1	MS-0734	E. Stechel, 6330
1	MS–1413	G. Heffelfinger, 8630
1	MS–0895	H. Jones, 8632
1	MS–0895	D. Haaland, 8632
1	MS–0895	A. Martino, 8632
1	MS–9292	S. Branda, 8621
1	MS–1411	M. Sinclair, 1816
1	MS–1245	J. Emerson, 2453

External (Electronic Copy)

Paul Savage
Department of Chemistry and Biochemistry
Brigham Young University
C-100 BNSN
Provo, Utah 84602-5700
paul_savage@byu.edu

This page is intentionally left blank